Bioconjugate Chemistry

Article

pubs.acs.org/bc

Design and Synthesis of Small-Molecule Fluorescent Photoprobes Targeted to Aminopeptdase N (APN/CD13) for Optical Imaging of Angiogenesis

Anke Hahnenkamp,[†] Michael Schäfers,[‡,§] Christoph Bremer,[†,§] and Carsten Höltke*[,†]

[†]Department of Clinical Radiology, Albert-Schweitzer-Campus 1/A16, University Hospital Muenster, D-48149 Muenster, Germany

[‡]European Institute of Molecular Imaging, Mendelstrasse 11, University of Muenster, D-48149 Muenster, Germany

[§]Interdisciplinary Center of Clinical Research, University of Muenster, D-48149 Muenster, Germany

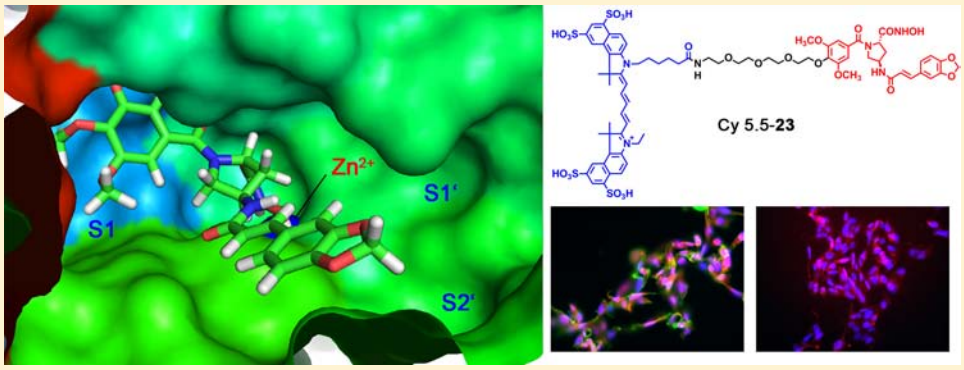

ABSTRACT: We report here the synthesis of a nonpeptide, small-molecule fluorescent imaging agent with high affinity to aminopeptidase N (APN/CD13), a key player in a variety of pathophysiological angiogenic processes. On the basis of a recently described lead structure, we synthesized three putative precursor compounds by introducing polyethylene glycol (PEG) spacers comprising amino groups for dye labeling. Different attachment sites resulted in substantial differences in target affinity, cell toxicity, and target imaging performance. In comparison to bestatin, a natural inhibitor of many aminopeptidases, two of our compounds (**22**, **23**) exhibit comparable inhibition potency, while a third (**21**) does not show any inhibiting effect. Cell binding assays with APN-positive BT-549 and APN-negative BT-20 cells and the final fluorescent probes Cy 5.5-**21** and Cy 5.5-**23** confirm these findings. The favorable characteristics of Cy 5.5-**23** will now be proven in in vivo experiments with murine models of high APN expression and may serve as a tool to better understand APN pathophysiology.

INTRODUCTION

Angiogenesis is a key factor in many pathophysiological processes such as tumor growth and formation of metastasis, myocardial remodeling after infarction, as well as diabetes or arthritis, where it is mainly triggered by the dysregulated release of growth factors, by hypoxia or by inflammation.[1,2] In addition to angiogenic signaling, tumor growth and progression needs extracellular proteases to degrade the surrounding extracellular matrix (ECM) and enable the sprouting of new vessels. Aminopeptidase N (CD13/APN) is a zinc-dependent ectoenzyme located in the outer cell membranes of various cell types. APN is mainly found on epithelial cells of the small intestine and the kidneys, where it is involved in digestive and regulative processes,[3,4] but APN has also been found upregulated in a number of human tumors, including ovarian cancer,[5,6] prostate cancer,[7,8] renal cell carcinoma,[9,10] and thyroid cancer,[11,12] where it was identified as an important mediator of tumor angiogenesis promoting progression, metastasis, and tumor cell survival.[13−15] Thus, APN could potentially serve as an attractive target for tumor imaging as well as targeted therapies.

APN exhibits a high affinity to peptides containing the amino acid motif asparagine−glycine−arginine (NGR), and recently, we were able to show that a cyclic NGR-containing peptide conjugated to the cyanine dye Cy 5.5 is capable of delineating APN expression in vivo using optical imaging techniques.[16] In contrast to peptides, synthetic compounds have the advantage of a higher bioavailability and a higher in vivo stability. Approaches toward peptidomimetics as ligands for APN aim at compounds that bind to the catalytic Zn^{2+} ion. Typical functional groups for chelating a doubly charged cation are e.g. hydroxamate, carboxylate, sulfhydryl, etc.

In this paper, we describe for the first time the synthesis of a nonpeptidic *trans*-4-amino-L-proline derivative conjugated to a fluorescent dye that can be exploited for noninvasive imaging of APN expression.

Received: February 6, 2013
Revised: April 24, 2013
Published: May 5, 2013

MATERIALS AND METHODS

General. All chemicals, reagents and solvents for the synthesis of the compounds were analytical grade and purchased from commercial sources. *trans*-4-Amino-*N*-Boc-L-proline methyl ester hydrochloride (**6**) was purchased from Alfa Aesar (Karlsruhe, Germany), bestatin, ferulic acid (**1**), syringic acid (**2**), 3,4-dimethoxycinnamic acid (**7**), and 3,4-methylenedioxycinnamic acid (**8**) were from Sigma-Aldrich (Schnelldorf, Germany), 2-(2-(2-(2-azidoethoxy)ethoxy)-ethoxy)ethyl methane sulfonate was synthesized according to literature procedures,[17] and lead compound **I2** (Figure 1) was

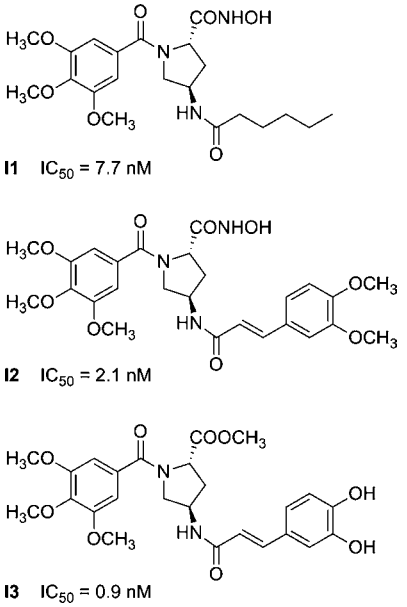

Figure 1. Benzoyl-aminoproline derivatives (**I1**–**I3**) introduced by Xu and Li in 2005 and the reported inhibition values. **I1** and **I2** contain caproic and dimethoxycinnamic acid amides, respectively, and a hydroxamic acid functional group, while **I3** contains a caffeic acid amide and a carboxylic ester functional group. All compounds are described to possess a high affinity to APN. We chose **I2** with an IC_{50} value of 2.1 nM as lead structure for further modification.

synthesized as reported.[18] ^{1}H NMR and ^{13}C NMR spectra were recorded on a Bruker ARX 300 or an AMX 400 (Bruker BioSpin GmbH, Rheinstetten, Germany), respectively. Major and minor signals from rotational isomers are given if an assignment was possible. Mass spectrometry was performed using a Bruker MALDI-TOF-MS Reflex IV (matrix: DHB, Bruker Daltonics GmbH, Bremen, Germany) or a QUATTRO LCZ (Waters Micromass, Manchester, UK) spectrometer with a nanospray capillary inlet. HPLC-purification was performed on a gradient RP-HPLC using a Knauer system with two K-1800 pumps, an S-2500 UV detector (Herbert Knauer GmbH, Berlin, Germany), and a RP-HPLC Nucleosil 100–5 C18 column (250 mm × 8.0 mm). Hydroxamic acid derivatives were purified as follows: λ = 254 nm; flow = 5.5 mL/min; eluents: A, water for injection/trifluoroacetic acid (TFA) 1000/1 (v/v); B, acetonitrile/TFA 1000/1 (v/v); elution gradient, 85% A for 1 min, from 85% to 15% A in 20 min, 15% A for 2 min, from 15% to 85% A in 1 min. The following conditions were used for purifying the fluorescently labeled derivatives: elution gradient, 95% A for 2 min, from 95% to 35% A in 18 min, 35% A for 1 min, from 35% to 95% A in 1 min. The recorded data was processed by the ChromGate HPLC software (Knauer).

Ferulic Acid Ethyl Ester. Ferulic acid (**1**) (19.4 g, 100 mmol) was dissolved in 350 mL of ethanol and treated with 30 mL (400 mmol) of thionyl chloride at 0 °C. After stirring overnight at room temperature, the solvent and excess thionyl chloride were removed by evaporation. Ethyl acetate was added, and the organic phase was washed with water (3 × 100 mL) and brine and dried over $MgSO_4$. Filtration and evaporation of the solvent yields 20.1 g (90.5 mmol, 90%) of the desired ester. ^{1}H NMR ($CDCl_3$, 300 MHz) δ = 7.61 (d, J = 16.1 Hz, 1H), 7.10–7.01 (m, 2H), 6.90 (d, J = 8.4 Hz, 1H), 6.29 (d, J = 16.1 Hz, 1H), 6.03 (br, 1H), 4.26 (q, J = 7.1 Hz, 2H), 3.92 (s, 3H), 1.33 (t, J = 7.1 Hz, 3H) ppm. ^{13}C NMR ($CDCl_3$, 75 MHz) δ = 167.4, 147.9, 146.8, 144.8, 126.9, 123.1, 115.6, 114.8, 109.3, 60.4, 55.9, 14.4 ppm.

(E)-3-(4-(2-(2-(2-(2-Azidoethoxy)ethoxy)ethoxy)ethoxy)-3-methoxyphenyl)acrylic Acid Ethyl Ester. To a solution of ferulic acid ethyl ester (2.85 g, 12.8 mmol) in 50 mL of DMF was added Cs_2CO_3 (6.51 g, 20.0 mmol) and 2-(2-(2-(2-azidoethoxy)ethoxy)ethoxy)ethyl methane sulfonate (4.16 g, 14.0 mmol). The mixture was heated to 80 °C overnight, cooled, and poured into water. After extraction with ethyl acetate, the combined organic fractions are washed with brine and dried over $MgSO_4$. Filtration and evaporation of the solvent yielded 5.95 g (12.0 mmol, 94%) of the desired PEG derivative. ^{1}H NMR ($CDCl_3$, 300 MHz) δ = 7.62 (d, J = 15.9 Hz, 1H), 7.10–7.03 (m, 2H), 6.90 (d, J = 7.8 Hz, 1H), 6.31 (d, J = 15.9 Hz, 1H), 4.39–4.36 (m, 2H), 4.25 (q, J = 7.5 Hz, 2H), 4.21 (t, J = 5.5 Hz, 2H), 3.90 (t, J = 5.5 Hz, 2H), 3.88 (s, 3H), 3.74–3.72 (m, 2H), 3.69–3.64 (m, 6H), 3.41–3.36 (m, 2H), 1.33 (t, J = 7.5 Hz, 3H) ppm. ^{13}C NMR ($CDCl_3$, 75 MHz) δ = 167.2, 150.4, 149.6, 144.5, 127.8, 122.4, 116.0, 113.1, 110.2, 70.9, 70.7, 70.6, 70.5, 70.0, 69.5, 68.4, 60.4, 55.9, 50.7, 14.3 ppm.

(E)-3-(4-(2-(2-(2-(2-Azidoethoxy)ethoxy)ethoxy)ethoxy)-3-methoxyphenyl)acrylic Acid ***2.*** An amount of 10.5 g (25.0 mmol) of the above ester was dissolved in a 3:1:1 mixture of THF/MeOH/water (250 mL). Lithium hydroxide (2.5 g 100 mmol) was added, and the mixture was stirred for 5 h at room temperature. The solvent was removed by evaporation and the residue taken up in water and acidified with 2.5 M HCl. Extraction with chloroform yielded a crude waxy solid which was purified by flash column chromatography (cyclohexane/ethyl acetate 1:2). Yield: 4.67 g (11.8 mmol, 47%). ^{1}H NMR ($CDCl_3$, 300 MHz) δ = 8.70 (br, 1H), 7.71 (d, J = 15.9 Hz, 1H), 7.14–7.05 (m, 2H), 6.91 (d, J = 8.4 Hz, 1H), 6.32 (d, J = 15.9 Hz, 1H), 4.25–4.21 (m, 2H), 3.94–3.90 (m, 2H), 3.89 (s, 3H), 3.76–3.72 (m, 2H), 3.71–3.65 (m, 8H), 3.41–3.36 (m, 2H) ppm. ^{13}C NMR ($CDCl_3$, 75 MHz) δ = 172.0, 150.7, 149.5, 146.6, 127.3, 122.8, 115.0, 112.8, 110.2, 70.7, 70.6 (2 signals), 70.5, 69.9, 69.4, 68.3, 55.8, 50.5 ppm.

Syringic Acid Ethyl Ester. Syringic acid (**3**) 9.91 g (50.0 mmol) was dissolved in 250 mL of ethanol and treated with 30 mL (400 mmol) of thionyl chloride at 0 °C. After stirring overnight at room temperature, the mixture was carefully added to an ice-cold saturated aqueous solution of $NaHCO_3$ until neutralization. After evaporation of most of the alcohol, ethyl acetate was added and the organic layer was separated. The aqueous layer was discarded; the organic layer was washed with brine and dried over $MgSO_4$. Filtration and evaporation of the solvent yielded 9.41 g (41.6 mmol, 83%) of the desired ester as a white crystalline solid. ^{1}H NMR ($CDCl_3$, 300 MHz) δ = 7.33

dx.doi.org/10.1021/bc400074w | *Bioconjugate Chem.* 2013, 24, 1027–1038

(s, 2H), 5.70 (br, 1H), 4.37 (q, J = 7.4 Hz, 2H), 3.94 (s, 6H), 1.40 (t, J = 7.4 Hz, 3H) ppm. ^{13}C NMR ($CDCl_3$, 75 MHz) δ = 166.3, 146.5, 139.0, 121.3, 106.5, 60.9, 56.3, 14.3 ppm.

4-(2-(2-(2-(2-Azidoethoxy)ethoxy)ethoxy)ethoxy)-3,5-dimethoxybenzoic Acid Ethyl Ester ***4***. An amount of 9.4 g of syringic acid ethyl ester (41.6 mmol) was dissolved in 150 mL of DMF. Cs_2CO_3 (20.3 g, 62.4 mmol) and 2-(2-(2-(2-azidoethoxy)ethoxy)ethoxy)ethyl methane sulfonate (13.4 g, 45.0 mmol) were added, and the mixture was stirred at 70 °C for 4 h. The main amount of DMF was evaporated at reduced pressure; the residue was suspended in ethyl acetate and successively washed with satd aq ammonium chloride solution and brine. After drying over $MgSO_4$ and filtration, the solvents were evaporated. Yield: 17.0 g, 39.8 mmol, 96%. ^{1}H NMR ($CDCl_3$, 300 MHz) δ = 7.29 (s, 2H), 4.37 (q, J = 7.2 Hz, 2H), 4.23−4.19 (m, 2H), 3.90 (s, 6H), 3.84−3.79 (m, 2H), 3.75−3.70 (m, 2H), 3.69−3.65 (m, 8H), 3.39 (t, J = 4.8 Hz, 2H), 1.40 (t, J = 7.2 Hz, 3H) ppm. ^{13}C NMR ($CDCl_3$, 75 MHz) δ = 166.1, 152.9, 141.0, 125.5, 106.6, 72.1, 70.5 (4 signals), 70.3, 69.9, 61.0, 56.0, 50.5, 14.2 ppm.

4-(2-(2-(2-(2-Aminoethoxy)ethoxy)ethoxy)ethoxy)-3,5-dimethoxybenzoic Acid Ethyl Ester. The above azide (11.0 g, 25.7 mmol) was dissolved in ethanol (150 mL), and a small portion of Pd/C (10%, Sigma-Aldrich) was added. The flask was evacuated and refilled with hydrogen. This procedure was repeated three times, and the mixture was stirred under a hydrogen atmosphere overnight. Filtration over Celite (acid-washed, Sigma-Aldrich) and evaporation of the solvent yielded 10.3 g (25.6 mmol, 99%) of the product as a clear oil. ^{1}H NMR ($CDCl_3$, 300 MHz) δ = 7.21 (s, 2H), 4.29 (q, J = 7.2 Hz, 2H), 4.15−4.10 (m, 2H), 3.81 (s, 6H), 3.75−3.71 (m, 2H), 3.67−3.53 (m, 11H), 3.45−3.41 (m, 1H), 3.35−3.29 (m, 1H), 2.80−2.75 (m, 1H), 1.31 (t, J = 7.2 Hz, 3H) ppm. ^{13}C NMR ($CDCl_3$, 75 MHz) δ = 165.9, 152.8, 141.0, 125.3, 106.4, 72.0, 71.3, 70.4 (2 signals), 70.3, 70.2, 70.1, 60.8, 55.9, 51.1, 14.1 ppm.

4-(2-(2-(2-(2-N-Boc-aminoethoxy)ethoxy)ethoxy)ethoxy)-3,5-dimethoxybenzoic Acid Ethyl Ester. The above amine (5.05 g, 12.6 mmol) was dissolved in a 1:1 mixture of MeOH and ^{t}BuOH (40 mL) and was treated with a solution of 3.27 g (15.0 mmol) of Boc_2O in ^{t}BuOH dropwise. The mixture was stirred overnight at room temperature, then the solvent was evaporated and the crude residue was purified by flash column chromatography (cyclohexane/ethyl acetate 1:1), yield 4.95 g (9.87 mmol, 78%). ^{1}H NMR ($CDCl_3$, 300 MHz) δ = 7.22 (s, 2H), 5.00 (br, 1H), 4.30 (q, J = 7.1 Hz, 2H), 4.16−4.11 (m, 2H), 3.82 (s, 6H), 3.76−3.72 (m, 2H), 3.68−3.63 (m, 2H), 3.61−3.52 (m, 6H), 3.46 (t, J = 4.8 Hz, 2H), 3.27−3.20 (m, 2H), 1.45 (s, 9H), 1.32 (t, J = 7.1 Hz, 3H) ppm. ^{13}C NMR ($CDCl_3$, 75 MHz) δ = 166.2, 156.0, 152.9, 141.0, 125.5, 106.6, 79.1, 72.2, 70.6 (2 signals), 70.5, 70.4, 70.2, 70.1, 61.0, 56.1, 40.3, 28.4, 14.3 ppm.

4-(2-(2-(2-(2-N-Boc-aminoethoxy)ethoxy)ethoxy)ethoxy)-3,5-dimethoxybenzoic Acid ***5***. The above ester (4.95 g, 9.87 mmol) was dissolved in a 3:1:1 mixture of THF/MeOH/water (50 mL). Lithium hydroxide (1.44g 60.0 mmol) was added, and the mixture was stirred overnight at room temperature. The solvent were removed by evaporation and the residue taken up in water and acidified with 2.5 M HCl. Extraction with chloroform yielded the product as a clear oil (4.64 g, 9.80 mmol, 99%). ^{1}H NMR ($CDCl_3$, 300 MHz) δ = 11.22 (br, 1H), 7.27 (s, 2H), 5.10 (br, 1H), 4.17−4.13 (m, 2H), 3.82 (s, 6H), 3.76−3.72 (m, 2H), 3.69−3.63 (m, 2H), 3.62−3.53 (m, 6H), 3.48 (t, J = 5.1 Hz, 2H), 3.29−3.21 (m, 2H), 1.36 (s, 9H) ppm. ^{13}C NMR ($CDCl_3$, 75 MHz) δ = 170.2, 156.0, 152.9, 141.5, 124.6, 107.0, 79.1, 72.1, 70.5 (2 signals), 70.4, 70.3, 70.0 (2 signals), 56.0, 40.2, 28.2 ppm.

(2S,4R)-N-Boc-4-((E)-3-(3,4-dimethoxyphenyl)acrylamido)-proline Methyl Ester ***9***. An amount of 760 mg (3.65 mmol) of 3,4-dimethoxycinnamic acid (**7**) was dissolved in toluene (25 mL) and treated with 1.45 mL (2.38 g, 20.0 mmol) of thionyl chloride. After refluxing for 4 h, the solvent and excess thionyl chloride were removed by evaporation (60 °C, 130 mbar). The residue was dissolved in chloroform and added dropwise to a solution of 1.00 g (3.56 mmol) of **6** and 1.56 mL (1.16 g, 9.00 mmol) of diisopropylethylamine (DIPEA) in 20 mL of chloroform at 0 °C. After stirring overnight at room temperature, the organic solution was successively washed with water, diluted hydrochloric acid, and brine and dried over $MgSO_4$. Filtration and evaporation of the solvent yielded 1.34 g of a yellow foam, which was purified by flash column chromatography (cyclohexane/ethyl acetate 1:1→1:2). Yield: 800 mg of the product as a white foam (1.87 mmol, 52%). ^{1}H NMR ($CDCl_3$, 300 MHz) δ = 7.57 (d, J = 15.9 Hz, 1H), 7.11−7.00 (m, 2H), 6.84 (d, J = 8.4 Hz, 1H), 6.46 (d, br, J = 6.4 Hz, 0.6H), 6.35 (m, 0.4H), 6.33 (d, J = 15.9 Hz, 1H), 4.74−4.60 (m, 1H), 4.43 (t, J = 7.0 Hz, 0.4H), 4.30 (t, J = 7.8 Hz, 0.6H), 3.90 (s, 3H), 3.89 (s, 3H), 3.85−3.77 (m, 1H), 3.75 (s, 1.8H), 3.72 (s, 1.2H), 3.54−3.47 (m, 0.6H), 3.43−3.35 (m, 0.4H), 2.47−2.36 (m, 0.6H), 2.32−2.22 (m, 1.4H), 1.46 (s, 3.6H), 1.43 (s, 5.4H) ppm. ^{13}C NMR ($CDCl_3$, 75 MHz, major) δ = 173.0, 166.0, 153.8, 150.6, 149.1, 141.3, 127.6, 122.1, 118.0, 111.1, 109.6, 80.7, 57.7, 55.9, 55.8, 52.3, 51.6, 48.3, 37.1, 28.2 ppm. ^{13}C NMR ($CDCl_3$, 75 MHz, minor) δ = 172.6, 165.9, 154.2, 150.6, 149.1, 141.4, 127.6, 122.0, 117.9, 111.1, 109.5, 80.7, 57.5, 55.9, 55.8, 52.1, 51.6, 48.7, 36.0, 28.3 ppm. HRMS (EI): m/z = 457.1937 $[M + Na]^+$ (calcd 457.1945), 891.3983 $[2M + Na]^+$ (calcd 891.3998), 1325.6004 $[3M + Na]^+$ (calcd 1325.6051).

(2S,4R)-N-Boc-4-((E)-3-(benzo[d][1,3]dioxol-5-yl)-acrylamido)proline Methyl Ester ***10***. An amount of 700 mg (3.64 mmol) of 3,4-methylenedioxycinnamic acid (**8**) was dissolved in toluene (30 mL) and treated with 1.45 mL (2.38 g, 20.0 mmol) of thionyl chloride. After refluxing for 3.5 h, the solvent and excess thionyl chloride were removed by evaporation (60 °C, 130 mbar). The residue was dissolved in chloroform and added dropwise to a solution of 1.00 g (3.56 mmol) of **6** and 1.56 mL (1.16 g, 9.00 mmol) of DIPEA in 20 mL of chloroform at 0 °C. After stirring overnight at room temperature, the organic solution was successively washed with water, diluted hydrochloric acid, and brine and dried over $MgSO_4$. Filtration and evaporation of the solvent yielded 1.32g of an off-white foam, which was purified by flash column chromatography (cyclohexane/ethyl acetate 1:1). Yield: 1.03 g of the product as a white foam (2.46 mmol, 70%). ^{1}H NMR ($CDCl_3$, 300 MHz) δ = 7.54 (d, J = 15.4 Hz, 1H), 7.00−6.95 (m, 2H), 6.79 (d, J = 8.9 Hz, 1H), 6.29−6.20 (m, 1.6H), 6.07−6.01 (m, 0.4H), 5.99 (s, 2H), 4.65 (br, 1H), 4.43 (t, J = 6.9 Hz, 0.4H), 4.31 (t, J = 7.4 Hz, 0.6H), 3.90−3.77 (m, 1H), 3.75 (s, 3H), 3.50 (dd, J = 11.1 Hz, J = 2.5 Hz, 0.6H), 3.37 (dd, J = 11.3 Hz, J = 4.0 Hz, 0.4H), 2.45−2.35 (m, 0.6H), 2.33−2.22 (M, 1.4H), 1.46 (s, 3.6H), 1.43 (s, 5.4H) ppm. ^{13}C NMR ($CDCl_3$, 75 MHz, major) δ = 173.0, 166.0, 153.8, 149.2, 148.3, 141.3, 129.1, 124.0, 118.3, 108.5, 106.3, 101.4, 80.7, 57.8, 52.2, 51.6, 48.4, 37.1, 28.3 ppm. ^{13}C NMR ($CDCl_3$, 75 MHz, minor) δ = 172.7, 167.2, 154.4, 149.6, 148.3, 141.5, 129.0, 124.3, 118.0, 108.5, 106.5, 101.5, 80.7, 57.5, 52.2, 51.6, 48.7, 35.9, 28.4 ppm.

HRMS (EI): m/z = 441.1637 [M + Na]$^+$ (calcd 441.1638), 859.3372 [2M + Na]$^+$ (calcd 859.3378), 1277.5097 [3M + Na]$^+$ (calcd 1277.5118).

(2S,4R)-N-Boc-4-((E)-3-((((4-azidoethoxy)ethoxy)ethoxy)-ethoxy-3-methoxybenzyl)-acrylamido)proline Methyl Ester ***11***. A solution of 1.60 g (4.00 mmol) **4**, 610 mg (4.50 mmol) hydroxybenzotriazole hydrate (HOBT·H_2O) and 1.45 g (4.50 mmol) 2-(1H-benzotriazole-1-yl)-1,1,3,3-tetramethyluronium tetrafluoroborate (TBTU) in 30 mL of DMF was treated with 1.22 mL (900 mg, 6.7 mmol) DIPEA and 1.00 g (3.56 mmol) of **6** at room temperature. After stirring for 30 min, another mL of DIPEA was added and the resulting mixture was stirred for additional 23 h. Ethyl acetate was added, and the organic phase was washed with diluted hydrochloric acid and brine. After drying and filtration, the solvent was removed by rotary evaporation and the residue was directly used in the next step. HRMS (ESI): m/z = 644.2904 [M + Na]$^+$ (calcd 644.2908).

(2S,4R)-4-((E)-3-(3,4-Dimethoxyphenyl)acrylamido)proline Methyl Ester Trifluoro-acetate ***12***. A solution of **9** (800 mg, 1.84 mmol) in 10 mL of CH_2Cl_2 was treated with TFA (5 mL in 5 mL of CH_2Cl_2) at 0 °C. After stirring overnight at room temperature, the solvent and excess TFA was removed by evaporation at reduced pressure. The remaining trifluoroacetate **12** was directly used in the next step.

(2S,4R)-4-((E)-3-(Benzo[d][1,3]dioxol-5-yl)acrylamido)-proline Methyl Ester Trifluoro-acetate ***13***. To a solution of 1.03 g (2.46 mmol) of **10** in CH_2Cl_2 was added a solution of 3.0 mL of TFA in 7.0 mL of CH_2Cl_2 at 0 °C. After stirring overnight at room temperature, the solvent and excess TFA was removed by rotary evaporation and the residue was taken up in 10 mL of methanol. The alcohol was evaporated, and the procedure was repeated twice. Yield: 1.04 g of an off-white foam (2.40 mmol, 98%). ^{1}H NMR (DMSO-d_6, 300 MHz) δ = 10.07 (br, 1H), 9.21 (br, 1H), 8.51 (d, J = 6.3 Hz, 1H), 7.37 (d, J = 15.6 Hz, 1H), 7.15 (d, J = 1.5 Hz, 1H), 7.06 (dd, J = 8.1 Hz, J = 1.5 Hz, 1H), 6.93 (d, J = 8.1 Hz, 1H), 6.41 (d, J = 15.6 Hz, 1H), 6.05 (s, 2H), 4.67−4.59 (m, 1H), 4.47−4.37 (m, 1H), 3.77 (s, 3H), 3.57 (dd, J = 12.0 Hz, J = 6.7 Hz, 1H), 3.16 (dd, J = 12.0 Hz, J = 4.6 Hz, 1H), 2.42−2.21 (m, 2H) ppm. ^{13}C NMR (DMSO-d_6, 75 MHz) δ = 168.9, 165.5, 158.6 (q, J = 36 Hz, TFA), 148.8, 148.1, 139.4, 129.1, 123.6, 119.4, 115.7 (q, J = 290 Hz, TFA), 108.7, 106.2, 101.6, 57.9, 53.2, 50.3, 48.1, 33.4 ppm.

(2S,4R)-4-((E)-3-((((4−2-Azidoethoxy)ethoxy)ethoxy)-ethoxy-3-methoxybenzyl)-acrylamido)proline Methyl Ester Trifluoroacetate ***14***. The above Boc-protected proline **11** was dissolved in 20 mL of CH_2Cl_2 and treated with 5 mL of TFA at 0 °C. After stirring overnight at room temperature, the solvent and excess TFA was removed by rotary evaporation. The foamy residue was directly used in the next step.

(2S,4R)-4-((E)-3-(3,4-Dimethoxyphenyl)acrylamido)-1-(3,5-dimethoxy-4-(((2-N-Boc-aminoethoxy)ethoxy)ethoxy)-ethoxybenzoyl)proline Methyl Ester ***15***. The above trifluoro-acetate **12** was taken up in DMF (10 mL) and combined with a solution of **5** (600 mg, 1.30 mmol), TBTU (515 mg, 1.60 mmol), HOBt·H_2O (220 mg, 1.60 mmol), and 260 mg (350 μL, 2.00 mmol) of DIPEA in DMF (10 mL). After stirring the mixture overnight at room temperature, most of the solvent was removed on a rotary evaporator and the residue was separated between water and ethyl acetate. The organic phase was successively washed with diluted hydrochloric acid, water, and brine and dried over $MgSO_4$. After filtration and evaporation, the residue was purified by flash column chromatography. Yield: 1.00 g (1.27 mmol, 69%). ^{1}H NMR ($CDCl_3$, 300 MHz) δ = 7.53 (d, J = 15.6 Hz, 1H), 7.18−7.11 (m, 1H), 7.10−7.05 (m, 1H), 7.03−7.01 (m, 1H), 6.84 (d, J = 8.3 Hz, 1H), 6.76 (s, 2H), 6.23 (d, J = 15.6 Hz, 1H), 5.11−5.03 (m, 1H), 4.90−4.81 (m, 1H), 4.68−4.61 (m, 1H), 4.17−4.12 (m, 2H), 3.91 (s, 3H), 3.90 (s, 3H), 3.89−3.84 (m, 5H), 3.83 (s, 6H), 3.82−3.77 (m, 2H), 3.73−3.69 (m, 2H), 3.69−3.65 (m, 2H), 3.65−3.58 (m, 4H), 3.55−3.50 (m, 2H), 3.33−3.27 (m, 2H), 2.69−2.52 (m, 1H), 2.07 (br, 1H), 1.43 (s, 9H) ppm. ^{13}C NMR ($CDCl_3$, 75 MHz) δ = 174.7, 169.3, 165.6, 156.0, 153.2, 150.7, 149.1, 141.6, 139.2, 130.3, 127.5, 122.3, 118.0, 111.0, 109.5, 105.0, 79.1, 72.3, 70.6 (2 signals), 70.5, 70.4, 70.2, 70.1, 58.5, 56.8, 56.3 (2 signals), 55.9, 52.9, 49.1, 40.3, 34.6, 28.4 ppm. HRMS (EI): m/z = 812.3571 [M + Na]$^+$ (calcd 812.3576).

(2S,4R)-4-((E)-3-(Benzo[d][1,3]dioxol-5-yl)acrylamido)-1-(3,5-dimethoxy-4-(((2-N-Boc-aminoethoxy)ethoxy)ethoxy)-ethoxybenzoyl)proline Methyl Ester ***16***. A solution of 1.21 g (2.55 mmol) of **5** in 20 mL of DMF was treated with 380 mg (2.80 mmol) of HOBt·H_2O, 900 mg (2.80 mmol) TBTU and 730 μL (543 mg, 4.2 mmol) of DIPEA. To this was added a solution of 1.18 g (2.46 mmol) of **13** and 1.0 mL (745 mg, 5.75 mmol) of DIPEA at 0 °C. After stirring overnight at room temperature, ethyl acetate was added and the organic phase was successively washed with water, diluted hydrochloric acid, and brine. The organic layer was dried over $MgSO_4$ and filtered. The solvent was evaporated and the residue was purified by flash column chromatography (5% MeOH in ethyl acetate), yielding 1.375 g of a white foam (1.78 mmol, 72%). ^{1}H NMR ($CDCl_3$, 300 MHz) δ = 7.67 (br, 1H), 7.36 (d, J = 15.6 Hz, 1H), 6.74−6.66 (m, 2H), 6.63 (s, 2H), 6.46 (s, 1H), 6.10 (d, J = 15.6 Hz, 1H), 5.95 (s, 2H), 5.28−5.18 (m, 1H), 5.06 (br, 1H), 4.80 (br, 1H), 4.03 (dd, J = 11.2 Hz, J = 4.5 Hz, 1H), 3.85 (s, 3H), 3.83−3.77 (m, 3H), 3.65 (s, 6H), 3.63−3.57 (m, 10H), 3.53 (t, J = 7.8 Hz, 2H), 3.34−3.26 (m, 2H), 2.54−2.28 (m, 2H), 1.43 (s, 9H) ppm. ^{13}C NMR ($CDCl_3$, 75 MHz) δ = 172.3, 170.1, 166.0, 156.0, 153.1, 149.0, 148.1, 140.6, 129.0, 124.0, 118.6, 108.3, 105.8, 104.9, 101.3, 79.2, 72.1, 70.6, 70.5, 70.2, 55.8, 52.6, 49.2, 40.3, 28.3 ppm (due to broadening the remaining signals could not be detected). HRMS (EI): m/z = 769.3262 [M + Na]$^+$ (calcd 796.3263).

(2S,4R)-4-((E)-3-(3-Methoxy-4-(((2-azidoethoxy)ethoxy)-ethoxy)ethoxyphenyl)acryl-amido)-1-(3,4,5-trimethoxybenzoyl)proline Methyl Ester ***17***. The above amino trifluoroacetate **14** was dissolved in CH_2Cl_2 (30 mL) and treated with 1.0 mL (0.73 g, 7.20 mmol) of triethylamine (TEA). Then a solution of 920 mg (4.00 mmol) of 3,4,5-trimethoxybenzoylchloride in 20 mL of CH_2Cl_2 was added at 0 °C. After stirring overnight at room temperature, the organic phase was extracted twice with diluted hydrochloric acid, water, and brine. Flash column chromatography (10% MeOH/ethyl acetate) yielded 1.75 g (2.44 mmol, 69%) of the product as a white foam. ^{1}H NMR ($CDCl_3$, 300 MHz) δ = 7.56 (d, 7.5 Hz, 1H), 7.43 (d, J = 15.9 Hz, 1H), 6.74 (s, 3H), 6.67 (s, 2H), 6.19 (d, J = 15.9 Hz, 1H), 5.20−5.13 (m, 1H), 4.82−4.75 (m, 1H), 4.18−4.13 (m, 2H), 4.07 (dd, J = 11.4 Hz, J = 4.5 Hz, 1H), 3.89−3.84 (m, 2H), 3.82 (s, 3H), 3.78−3.70 (m, 6H), 3.70−3.62 (m, 10H), 3.66 (s, 6H), 3.37 (t, J = 5.2 Hz, 2H), 2.56−2.28 (m, 2H), 2.00−1.90 (m, 1H) ppm. ^{13}C NMR ($CDCl_3$, 75 MHz) δ = 172.3, 169.9, 166.2, 152.9, 149.8, 149.3, 141.0, 140.3, 129.6, 127.8, 121.7, 118.3, 112.8, 110.1, 105.0, 70.8, 70.6, 70.5, 70.0, 69.4, 68.3, 67.9, 60.6, 58.0, 57.4, 55.9, 55.7, 52.6, 50.6, 49.4, 35.1 ppm. HRMS (EI): m/z = 796.3262 [M + Na]$^+$ (calcd 796.3269).

(2S,4R)-4-((E)-3-(3-Methoxy-4-(((2-aminoethoxy)ethoxy)ethoxy)ethoxyphenyl)acryl-amido)-1-(3,4,5-trimethoxybenzoyl)proline Methyl Ester ***18.*** To a solution of **17** (1.30 g, 1.80 mmol) in 20 mL of THF was added 1.05 g (4.00 mmol) of triphenylphosphine, and the mixture was stirred for 1 h at room temperature. Then 100 μL of water were added, and the resulting mixture was stirred for additional 48 h. The solvent was evaporated, and the residue was purified by flash column chromatography (ethyl acetate → ethyl acetate/MeOH 4:1 + 2% TEA), yielding 1.19 g of a clear oil (1.70 mmol, 96%). ^{1}H NMR ($CDCl_3$, 300 MHz) δ = 7.82 (d. J = 7.6 Hz, 1H), 7.42 (d, J = 15.7 Hz, 1H), 6.74 (s, 3H), 6.66 (s, 2H), 6.21 (d, J = 15.7 Hz, 1H), 5.17 (t, J = 8.5 Hz, 1H), 4.78 (s, 1H), 4.15 (t, J = 4.6 Hz, 2H), 4.07 (dd, J = 11.2 Hz, J = 4.4 Hz, 1H), 3.86 (t, J = 4.7 Hz, 2H), 3.82 (s, 3H), 3.75−3.59 (m, 21H), 3.51 (t, J = 5.1 Hz, 2H), 2.86 (t, J = 5.1 Hz, 2H), 2.56−2.46 (m, 1H), 2.40−2.30 (m, 1H), 2.27 (br, 2H) ppm. ^{13}C NMR ($CDCl_3$, 75 MHz) δ = 172.2, 169.8, 166.2, 152.8, 149.7, 149.3, 140.7, 140.2, 129.5, 127.9, 121.5, 118.5, 112.8, 110.1, 105.0, 73.0, 70.7, 70.5, 70.4, 70.2, 69.4, 68.3, 60.6, 58.0, 57.3, 55.8, 55.6, 52.6, 49.4, 41.6, 35.0 ppm. HRMS (ESI): m/z = 690.3235 $[M + H]^+$ (calcd 690.3233), 712.3047 $[M + Na]^+$ (calcd 712.3052).

General Procedure for the Synthesis of Hydroxamic Acids from Methyl Esters. Powdered KOH (840 mg, 15.0 mmol) was dissolved in 15 mL of MeOH under argon. In a separate flask, 700 mg (10.0 mmol) of $NH_2OH{\cdot}HCl$ was dissolved in 10 mL of MeOH under argon. Both solutions were briefly refluxed and then cooled to below 40 °C. The KOH solution was transferred into the NH_2OH solution, and the mixture was stirred for 1 h at 40 °C. KCl was allowed to precipitate, and the supernatant solution was transferred into a solution of the methyl ester (1−2 mmol) in MeOH. The resulting mixture was stirred at room temperature for 24 h, then the solvent was evaporated and the residue was taken up in diluted hydrochloric acid and extracted with ethyl acetate. The combined organic portions are washed with brine, dried ($MgSO_4$), and filtered, and the solvent was evaporated.

(2S,4R)-4-((E)-3-(3-Methoxy-4-(((2-aminoethoxy)ethoxy)ethoxy)ethoxyphenyl)acryl-amido)-1-(3,4,5-trimethoxybenzoyl)proline Hydroxamic Acid ***21.*** From 1.19 g (1.70 mmol) of the methyl ester **18** an amount of 686 mg (1.00 mmol, 59%) of the product **21** could be isolated after purification by HPLC (conditions see above). HRMS (ESI): m/z = 691.3179 $[M + H]^+$ (calcd 691.3185).

(2S,4R)-4-((E)-3-(3,4-Dimethoxyphenyl)acrylamido)-1-(3,5-dimethoxy-4-(((2-amino-ethoxy)ethoxy)ethoxy)-ethoxybenzoyl)proline Hydroxamic Acid ***22.*** From 900 mg (1.14 mmol) of the methyl ester **15** an amount of 599 mg (753 μmol, 65%) of the Boc-protected intermediate **19** was isolated. HRMS (ESI): m/z = 813.3507 $[M + H]^+$ (calcd 813.3534). Deprotection with TFA in CH_2Cl_2 for 24 h at room temperature yielded 600 mg (745 μmol, 99%) of the amino trifluoroacetate hydroxamic acid derivative **22**. For conjugation, the compound can be purified by HPLC. HRMS (ESI): m/z = 691.3192 $[M + H]^+$ (calcd 691.3185).

(2S,4R)-4-((E)-3-(Benzo[d][1,3]dioxol-5-yl)acrylamido)-1-(3,5-dimethoxy-4-(((2-amino-ethoxy)ethoxy)ethoxy)-ethoxybenzoyl)proline Hydroxamic Acid ***23.*** From 570 mg (737 μmol) of the methyl ester **16** an amount of 560 mg (702 μmol, 95%) of the Boc-protected intermediate **20** was isolated. HRMS (ESI): m/z = 797.3186 $[M + H]^+$ (calcd 797.3216). Deprotection with TFA in CH_2Cl_2 for 24 h at room temperature yielded the amino trifluoroacetate hydroxamic acid derivative **23**. After purification by HPLC, an amount of 337 mg can be isolated (58%). HRMS (ESI): m/z = 675.2868 $[M + H]^+$ (calcd 675.2872).

Fluorescent Labeling of Amino-PEG Derivatives. Amino derivatives **21** and **23** were chosen for labeling experiments. An amount of 0.7 mg (1.0 μmol) of **21** or **23**, respectively, were dissolved in 100 μL of DMSO and transferred into 700 μL of 0.1 M $NaHCO_3$ buffer of pH 8.8. To these solutions were added 1.1 mg (1.0 μmol) of Cy 5.5 NHS ester dissolved in 200 μL of DMSO. After shaking for 4 h at room temperature, the mixtures were transferred into the HPLC system and purified using the same setup as for the hydroxamic acid derivatives (see above). The desired fractions were collected, and after evaporation of the solvent the residues were reconstituted in PBS. The identities of the conjugates were proven by mass spectrometry. HRMS of Cy 5.5-**21** (ESI): m/z = 1589.47805 $[M + H]^+$ (calcd 1589.47547). HRMS of Cy 5.5-**23** (ESI): m/z = 1573.44804 $[M + H]^+$ (calcd 1573.44417). The concentrations of the tracers were determined by photometric measurements using a Hitachi U-3010 spectrophotometer (Hitachi High-Technologies Europe GmbH, Mannheim, Germany). At least five different concentrations of the reconstituted solutions were measured at a wavelength of 676 nm. After recording the absorption values, the concentrations were determined employing Lambert−Beer's law (absorption coefficient ε_λ = 250.000 L·mol^{-1}·cm^{-1}).

Cell Lines and Reagents. Human breast cancer cells BT-20 (ATCC: HTB-19; Manassas, VA) were cultured in Gibco's MEM (Invitrogen, San Diego, CA) supplemented with 10% fetal calf serum (FCS), 1% penicillin and streptomycin, 1% glutamine, 1% nonesential amino acids, 1% Na-pyruvate, and 18.8 mM $NaHCO_3$. Human BT-549 cells (ATCC: HTB-122; Manassas, VA) were cultured in ATCC-formulated RPMI-1640 medium supplemented with 0.023 μU/mL insulin (Sigma-Aldrich Biochemie GmbH, Hamburg, Germany) and 10% FCS. Cells were grown routinely in a monolayer culture at 37 °C in a 5% CO_2 humidified air atmosphere. For flow and immunocytometry, a monoclonal antibody specific for human APN (antiCD13-FITC, AM 00642FC-N/ABIN263533 Acris Antibodies, Herford, Germany) was used (FITC = fluorescein isothiocyanate). Primer for RT-PCR were designed for human APN; fwd, CAGGACGCCACCTCTACCAT; rev, GAAGGAGAACGAGCCACCAC (product 126 bp) and housekeeping gene human β-actin (BC002409); fwd, CTGGGACGACATGGAGAAAA; rev, AAGGAAGGCTGGA-AGAGTGC (Eurofins MWG Operon, Ebersberg, Germany). APN substrate L-alanine-4-methyl-7-coumarinylamido trifluoroacetate (MCA) was from Sigma-Aldrich Biochemie GmbH, Hamburg, Germany.

Cell Toxicity/Growth Inhibition. Cells (1×10^5) were seeded in 4-well plates and incubated at 37° (5% CO_2) overnight (conditions see above). Different concentrations (10 μM, 50 μM, 150 μM, and 300 μM) of **21**, **22**, and **23**, respectively, or 300 μM of free cyanine dye Cy 5.5 were added and incubation was maintained for 4 days. After three days, culture media were exchanged by fresh media including inhibitors or dye. The cell numbers were determined by trypan-blue staining and Neubauer chamber counting every 24 h and compared to those without inhibitor.

Flow Cytometry. Cultured cells were washed with PBS (Ca^{2+}/Mg^{2+}), harvested with trypsin, resuspended, centrifuged (3 min at 500*g*) and washed again with PBS (Ca^{2+}/Mg^{2+}). Aliquots of 2.5×10^5 cells were blocked with PBS/BSA (0,1%)

Scheme 1. PEG Modification of Aromatic Building Blocks[a]

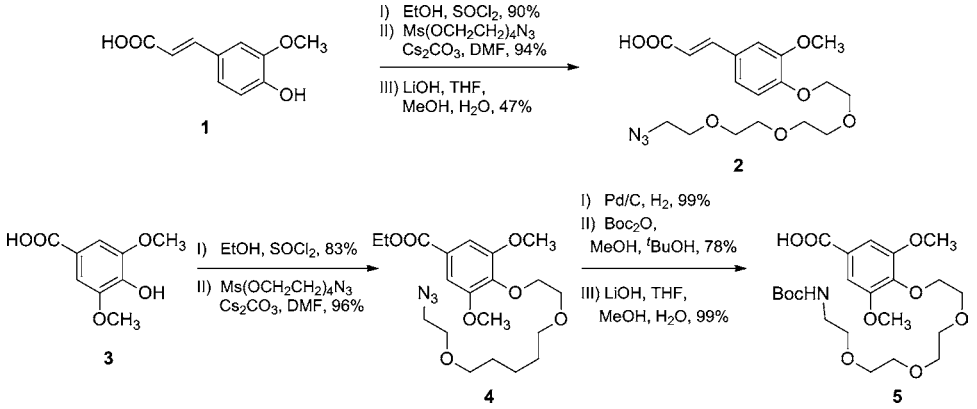

[a]Compounds **2** and **5** were synthesized beginning with commercially available starting material ferulic (**1**) and syringic acid (**3**), respectively. The key step is the installation of the PEG spacer by utilizing $Ms(OCH_2CH_2)_4N_3$, which has been introduced earlier.[17] Yields are given as isolated yields.

for 15 min at 4 °C, washed twice with PBS (Ca^{2+}/Mg^{2+}), and resuspended in 150 μL of binding buffer (150 mM NaCl, 10 mM $MgCl_2$, 10 mM $CaCl_2$, 0.5 mM $MnCl_2$, pH 7.2, diluted 1:20 in PBS/BSA 0,1%). Antibodies (AM 00642FC-N, Acris Antibodies, Herford, Germany; 1 μg/1 Mio cells) and propidium iodide (AnaSpec, Liege, Belgium; 1 μL/200 μL sample) were added and incubated for 45 min at 4 °C in the dark. Cells were washed, resuspended in PBS/BSA (0.1%), and analyzed on a CyFlow Space (Partec, Münster, Germany). Distribution of cells according to their fluorescence (FL1) intensity were documented; FL1 < 1 no specific binding.

RNA Isolation and RT-PCR. Total RNA was isolated from freshly harvested cells by using RNA Isolation Kit (RNeasy Mini Kit, Qiagen GmbH, Hilden, Germany). RNA concentration was estimated by Nanodrop spectrophotometer measurements (PEQLAB Biotechnologie GmbH, Erlangen, Germany). APN/CD13 expression was analyzed by using OneStep RT-PCR Kit (Qiagen GmbH, Hilden, Germany) following the instructions of the manufacturer. PCR-Programm: 50 °C for 30 min, 95 °C for 15 min (94 °C for 30 s, 55−57 °C for 30 s, 72 °C for 1 min), 30 cycles, 72 °C for 1 min. The products were analyzed by 1% agarose gel electrophoresis.

Immunocytometry. First, 50000 cells/100 μL were seeded on slides, incubated at 37° (5% CO_2) overnight, washed with PBS, and incubated in fixation solution (4% Formalin, room temperature, 10 min). After washing with PBS, the cells were then incubated in blocking solution (PBS/BSA, 0.1%, 15 min, room temperature), washed twice in PBS (Ca^{2+}/Mg^{2+}), and preincubated in binding buffer (50 mM NaCl, 10 mM $MgCl_2$, 10 mM $MnCl_2$, pH 7.2). The cells were incubated with the antibody (1:100) at room temperature for 45 min and washed with PBS. Nuclear counterstaining was performed with 4′,6-diamidino-2-phenylindole (DAPI). Staining procedures in the absence of the antibody and in the presence of control IgG_1, respectively, served as controls. Immunofluorescence was evaluated using a fluorescence microscopy (20× objective magnification, Nikon TE 2000-S). The microscope was equipped with a mercury vapor lamp, 377/447, 480/535, and 620/775 nm (excitation/emission) filters (DAPI, FITC and Cy 5.5, respectively), a Nikon DXM1200F camera, and Nikon's NIS-Elements software (Nikon, Tokyo, Japan).

In Vitro CD13/APN Tracer Binding Studies on Cells. First, 50000 cells/100 μL were incubated on slides in culture medium overnight. For binding studies, cells were washed with PBS and fixated (PBS with 4% formaldehyde) for 10 min at room temperature, washed, blocked (PBS/BSA 0.1%) for 15 min, washed twice ($PBS/Ca^{2+}/Mg^{2+}$), and preincubated in binding buffer (150 mM NaCl, 10 mM $MgCl_2$, 10 mM $CaCl_2$, 0.5 mM $MnCl_2$, pH 7.2, 1 min, room temperature). Binding buffer was removed, and 100 μL/well of fluorescent tracer or Cy 5.5 alone (2 μM, PBS) were added. After an incubation period of 4 h at room temperature, cells were washed, stained with DAPI (counterstain), washed again, and Fluoromount (Sigma Aldrich, St. Louis, MI) and cover slides were added. For blocking studies, cells were washed with PBS twice and treated with 333 μM concentration of bestatin in binding buffer for 10 min. The blocking solution was removed, and 100 μL/well of fluorescent tracer (2 μM, PBS) were added. After an incubation period of 1 h at room temperature, cells were washed again with $PBS/Ca^{2+}/Mg^{2+}$, and Fluoromount (Sigma Aldrich, St. Louis, MI) and cover slides were added. Cells could be directly visualized by fluorescence microscopy.

APN/CD13 Activity Assay. Activity and inhibition of surface aminopeptidase was measured on adherent BT-549 cells utilizing MCA as fluorogenic APN substrate.[19] A number of 2×10^4 cells/well were plated in a 96-well plate (Lumox Multiwell, Greiner Bio-One GmbH, Frickenhausen, Germany). After 24 h of recovering in culture medium, cells were washed with PBS and incubated with 100 μM MCA in PBS with 0.5% BSA and 20 mM HEPES (pH 7.2). The release of fluorescent product 7-amino-4-methylcoumarin was monitored on a Kodak Gel Logic 200 imaging system (Carestream Health Inc., Rochester, NY), with λ_{exc} = 360 nm and λ_{em} = 460 nm after 60 min. To assay for inhibition of enzymatic activity due to binding of new designed CD13/APN inhibitors, cells were pretreated in assay buffer containing different amounts (5×10^{-7} to 4×10^{-4} M) of the inhibitor at 37 °C for 30 min.

Data and Statistics. Cell numbers from cell growth inhibition experiments were determined from 3−4 different wells, and the means, standard deviations, and standard errors were calculated. Data from enzyme inhibition assays were processed by GraphPad Prism 4.0 software, and IC_{50} values were determined by nonlinear regression analysis using a one-site competition model. All results are presented as mean ± SEM.

dx.doi.org/10.1021/bc400074w | *Bioconjugate Chem.* 2013, 24, 1027−1038

Scheme 2. Synthetic Route to Carboxylic Acid Esters 15, 16, and 18[a]

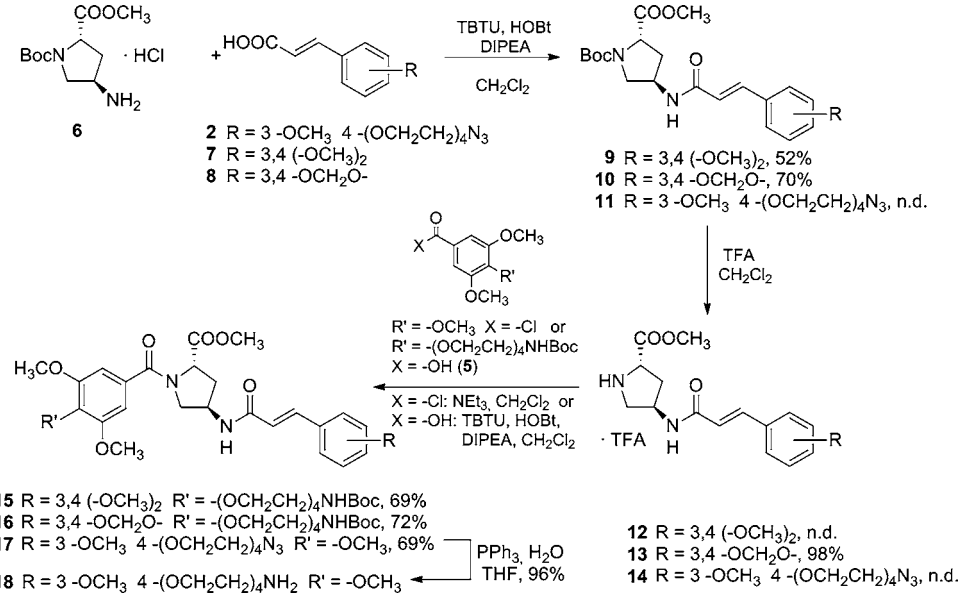

[a]Starting from *trans*-4-amino-*N*-Boc-L-proline methyl ester hydrochloride (**6**), the caffeic acid building blocks and the benzoyl building blocks are successively installed. Yields are given as isolated yields (n.d. = not determined).

Scheme 3. Final Conversion of the Carboxylic Acid Esters to the Hydroxamic Acids 21, 22, and 23[a]

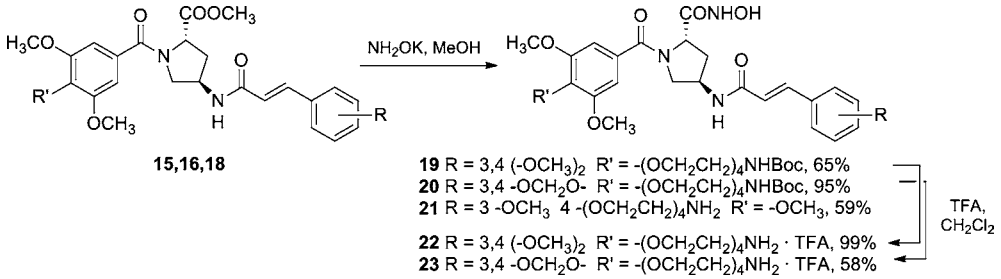

[a]For the transformation of the methyl esters to the hydroxamic acids, a protocol adapted from Fieser and Fieser[48] was used, employing a methanolic solution of NH_2OK. Final deprotection of *N*-Boc-protected hydroxamates **19** and **20** then yields amino−PEG hydroxamic acids **22** and **23**. Yields are given as isolated yields, except yield of compound **23** (after HPLC purification).

RESULTS

Chemistry. This work aimed at the synthesis of different 4-cinnamamido-1-(benzyloxy)proline derivatives as fluorescent biomarkers for the detection of aminopeptidase N (APN). For labeling purposes, we assembled a short polyethylene glycol (PEG) spacer with an amino group as the coupling site on either the benzoyl or the cinnamoyl residue of the lead structure. We therefore synthesized PEG-modified cinnamoyl derivative **2** and PEG-modified benzoyl derivative **5** (Scheme 1), which were then coupled to the proline ring on the 1- or 4-position, respectively. Both compounds were modified using 2-(2-(2-(2-azidoethoxy)ethoxy)ethoxy)ethyl methane sulfonate.[20] In further steps *trans*-4-amino-*N*-Boc-L-proline methyl ester hydrochloride **6** was coupled to cinnamic acid derivatives 3,4-dimethoxycinnamic acid **7**, 3,4-methylenedioxycinnamic acid **8**, or azido-PEG-derivative **2**, yielding aminoproline amides **9**−**11**. Deprotection with TFA in CH_2Cl_2 then yielded amines **12**−**14**, which were further coupled with 3,4,5-trimethoxybenzoylchloride or syringic acid derivative **5** to give aminoproline bisamides **15**−**17**. The azide function of **17** was further modified by Staudinger reduction to yield amine **18** (Scheme 2). For the transformation of the methyl esters to the hydroxamic acids, a protocol adapted from Fieser and Fieser[48] was used, employing a methanolic solution of NH_2OK. Final deprotection of *N*-Boc-protected hydroxamates **19** and **20** then yielded amino-PEG hydroxamic acids **22** and **23**. Together with amino-PEG hydroxamate **21**, a total of three different precursor compounds were synthesized which were directly used for dye conjugation (Scheme 3). We chose compounds **21** and **23** for labeling experiments. After purification by HPLC, we reconstituted the conjugates Cy 5.5-**21** and Cy 5.5-**23** (Figure 2) in PBS buffer for further in vitro experiments.

Target Identification. We determined the APN-expression of BT-549 and BT-20 cells by immunocytometry, FACS analysis, and RT-PCR (Figure 3). The strong binding of the specific monoclonal antibody *AM 00642FC-N* to BT-549 cells identified a high amount of target on the cell surface, whereas very low binding of this antibody to BT-20 cells was observed. This is in accordance with FACS analysis, which shows that more than 90% of BT-549 cells show a high binding of the antibody compared to only 0.02% of BT-20 cells. Also, *RT-PCR* examination of the cells reveals a high amount of *hAPN* in BT-549 cells, whereas BT-20 cells do not express this gene.

dx.doi.org/10.1021/bc400074w | *Bioconjugate Chem.* 2013, 24, 1027−1038

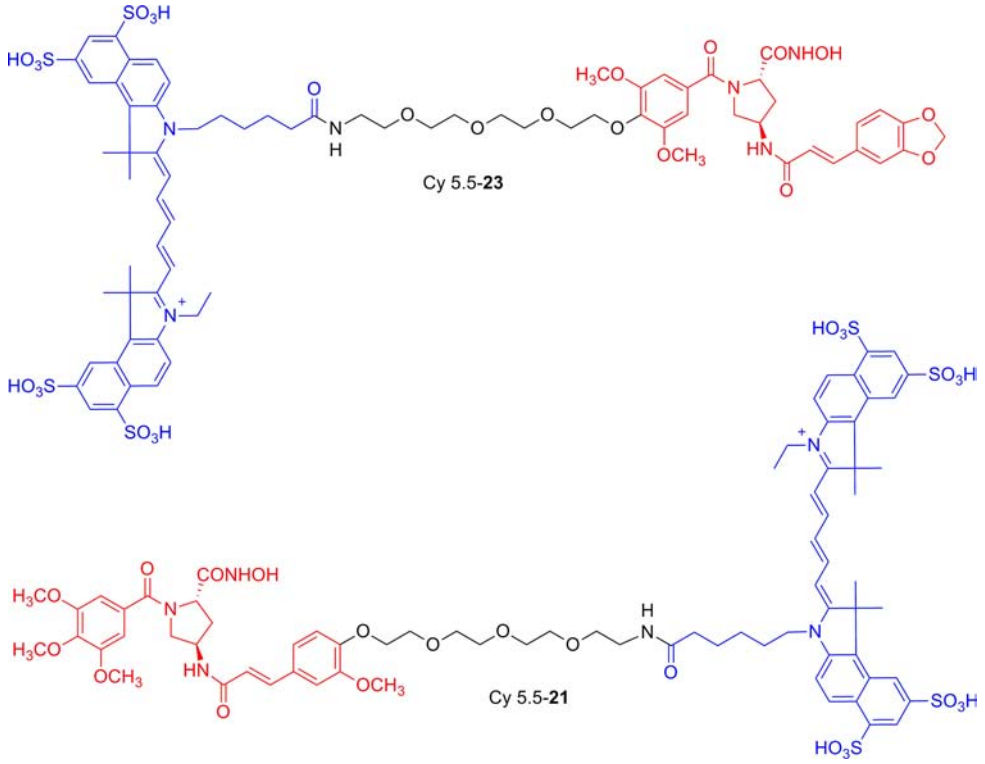

Figure 2. Structure of the differently substituted fluorescent tracers Cy 5.5-**21** and Cy 5.5-**23**. The ligand is displayed in red color, the PEG spacer in black, and the fluorescent dye Cy 5.5 in blue.

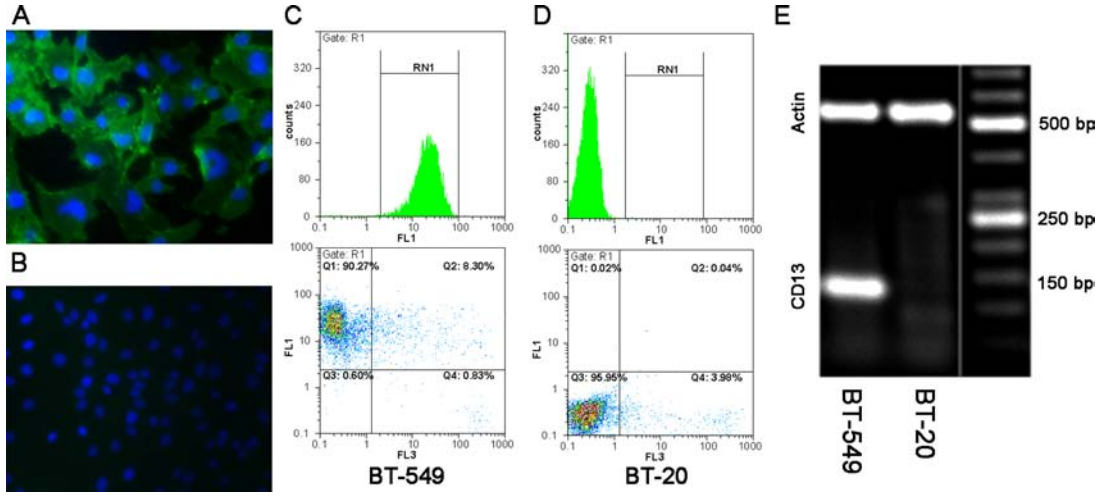

Figure 3. Target expression analysis of human breast cancer cell lines BT-549 and BT-20. (A,B) Immunocytometry on BT-549 (A) and BT-20 (B) cells using a FITC-labeled monoclonal antibody against human APN. (C,D) FACS analysis of BT-549 (C) and BT-20 (D) cells. The same antibody as in immunocytometry experiments was used. (E) Agarose gel visualization of *RT-PCR* examination of RNA from BT-549 and BT-20 cells. All experiments confirm a high target expression in BT-549 cells and negative results for BT-20 cells.

Inhibition Assays. Enzyme inhibition assays show a pronounced difference in the effects of **21**, **22**, and **23**. The regression curves are displayed in Figure 4A, and the results are displayed in Table 1. For comparison, known values from the literature are given for lead compound **I2** and bestatin. Compounds **22** and **23** show micromolar inhibition values comparable to the lead **I2** and bestatin, while **21** only shows a negligible value.

Cell Toxicity. The toxic effects of increasing concentrations of compounds **21**–**23** on cell growth and survival were examined on BT-549 and BT-20 cells (Figure 4B,C) and compared to a control and the applied fluorescent dye Cy 5.5 alone. Especially after 96 h, there was an obvious difference in the effects of **22** and **23** from that of **21**. Compounds **22** and **23** show a well-defined stepwise concentration-dependent decrease in cell number. Compound **21** has a more toxic effect on cells; after incubation with a concentration of 150 μM no vital BT-549 cells remain. Incubating BT-20 cells results in a different pattern. In this case, none of the inhibitors causes a marked toxic (i.e., growth-inhibiting) effect. The cyanine dye Cy 5.5 does not show a marked toxic effect on BT-549 cells, the cell number of BT-20 cells is decreased by 30%.

dx.doi.org/10.1021/bc400074w | *Bioconjugate Chem.* 2013, 24, 1027–1038

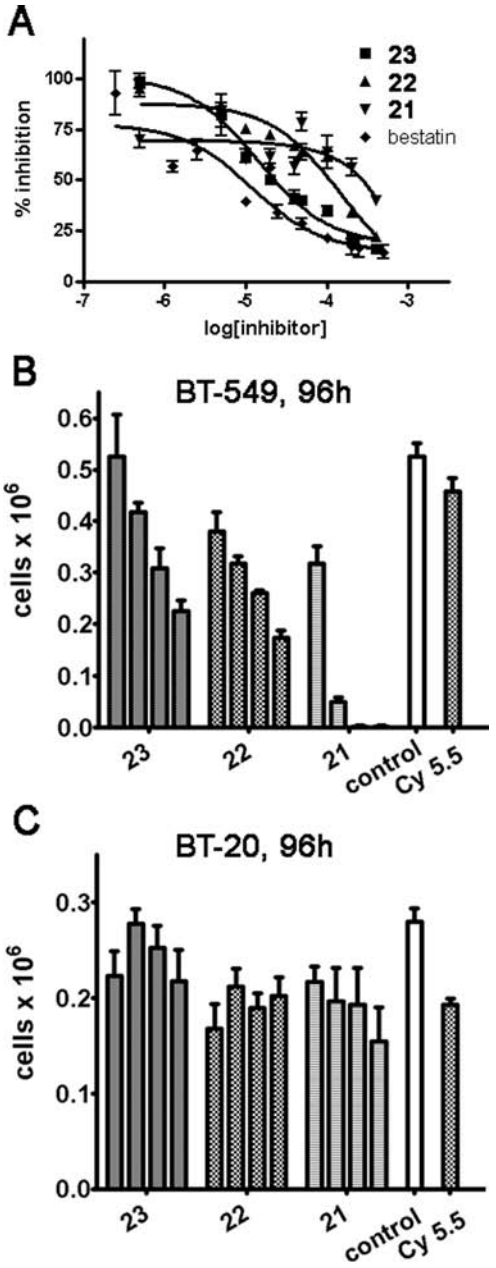

Figure 4. (A) Results of enzyme inhibition assays. Nonlinear regression analysis of the effect of compounds **21**−**23** and bestatin on MCA turnover of BT-549 cells yield IC_{50} values in the micromolar range for **22**, **23**, and bestatin; a value for compound **21** could not be determined. (B,C) Cell growth inhibition analysis of selected compounds on human breast cancer cell lines BT-549 and BT-20. Cell number after coincubation of cells with APN inhibitors **21**−**23** in increasing concentrations (10, 50, 150, and 300 μM, left to right) is shown (mean ± SEM). In addition, cell number without any inhibitor and cell number after incubation with 300 μM Cy 5.5 is displayed. Compound **21** is found to behave differently compared to **22** and **23**. While incubation of BT-549 cells with **22** and **23** shows a well-defined stepwise concentration-dependent decrease in cell number, compound **21** has a more toxic effect on cells; after incubation with a concentration of 150 μM, no vital cells remain. Incubating BT-20 cells results in a different pattern. In this case, no inhibitor exhibits any marked toxic effect. Also, the dye Cy 5.5 only shows marginal effects on cell growth on either cell line.

Cell Binding Assays. Fluorescent labeling of precursor compounds **21** and **23** was performed with Cy 5.5 NHS-ester.

Table 1. Determined Affinity Values of Our Synthesized Compounds to APN in Comparison to Those Reported in the Literature

compd	IC_{50} (APN) (μM)	lit.
I2	63.9	2.1 nM[31]
21	>500	
22	149.2	
23	14.3	
bestatin	12.0	13.1 μM[47]

In cell binding assays, Cy 5.5-**23** shows binding to APN-positive BT-549 cells (Figure 5A,D) but not to APN-negative BT-20 cells (Figure 5C,F). Also, we found that Cy 5.5-**21** does not bind to BT-549 cells, as shown in Figure 5B,E. The binding specificity of Cy 5.5-**23** can be concluded from the absence of binding of Cy 5.5 alone to BT-549 (Figure 5G, Cy 5.5; 5K, Cy 5.5/DAPI merge) and BT-20 cells (Figure 5H, Cy 5.5;5L, Cy 5.5/DAPI merge) and from predosing experiments with bestatin. While Cy 5.5-**23** strongly binds to BT-549 cells in the absence of bestatin (Figure 5E,F), its binding is inhibited with 100-fold excess of bestatin (Figure 5G,H).

DISCUSSION

Angiogenic vessels have become a popular target for molecular imaging approaches as well as targeted therapies in recent years.[21] Especially the vascular endothelial growth factor (VEGF) and its receptors (VEGFRs) have been frequently used as targets for various imaging approaches. Backer et al. designed a recombinant single-chain VEGF protein which could be labeled with either ^{99m}Tc, ^{64}Cu, or fluorescent dye Cy 5.5 and performed SPECT, PET, and optical imaging in mouse models of breast cancer.[22] Another prominent target for molecular imaging of angiogenesis are integrins (e.g., $\alpha_v\beta_3$[21,23]). Phage display techniques revealed a characteristic feature of integrins, including $\alpha_v\beta_3$, which is its high affinity to the amino acid motif arginine-glycine-aspartate, RGD.[24] Small peptides containing the RGD sequence have therefore been used as vehicles to target integrins in molecular imaging approaches.[25−27] [^{18}F]Galacto-RGD, a pharmacokinetically optimized cyclic peptide conjugate for PET imaging, has even been applied clinically.[28]

Aminopeptidase N (APN/CD13) is becoming more and more prominent as another key player in angiogenic processes. Especially in many human cancers, APN has been shown to be overexpressed on the cell surface of tumor cells, but also in murine infarction models, a 20-fold up-regulation of APN in the angiogenic infarct border was found compared to nonischemic control tissue, emphasizing its relevance in nontumor-associated pathological angiogenesis.[29] Natural and synthetic inhibitors of APN have recently been reviewed.[30,31] Bradykinin and substance P are natural peptides capable of inhibiting APN in micromolar concentrations. The most widely used compound is bestatin (Ubenimex), a dipeptidic compound first isolated from *Streptomyces olivoreticuli*. Bestatin exhibits inhibitory effects on several aminopeptidases, including APN, leucin aminopeptidase (LAP), and leukotriene A4 hydrolase, and is therefore a rather unspecific inhibitor. A multicenter, double blind, randomized phase III clinical study using bestatin in patients with stage I squamous-cell lung carcinoma has been completed in 2003. The administration of bestatin as a postoperative, adjuvant treatment was associated with a prolonged survival of patients with completely resected

dx.doi.org/10.1021/bc400074w | *Bioconjugate Chem.* 2013, 24, 1027−1038

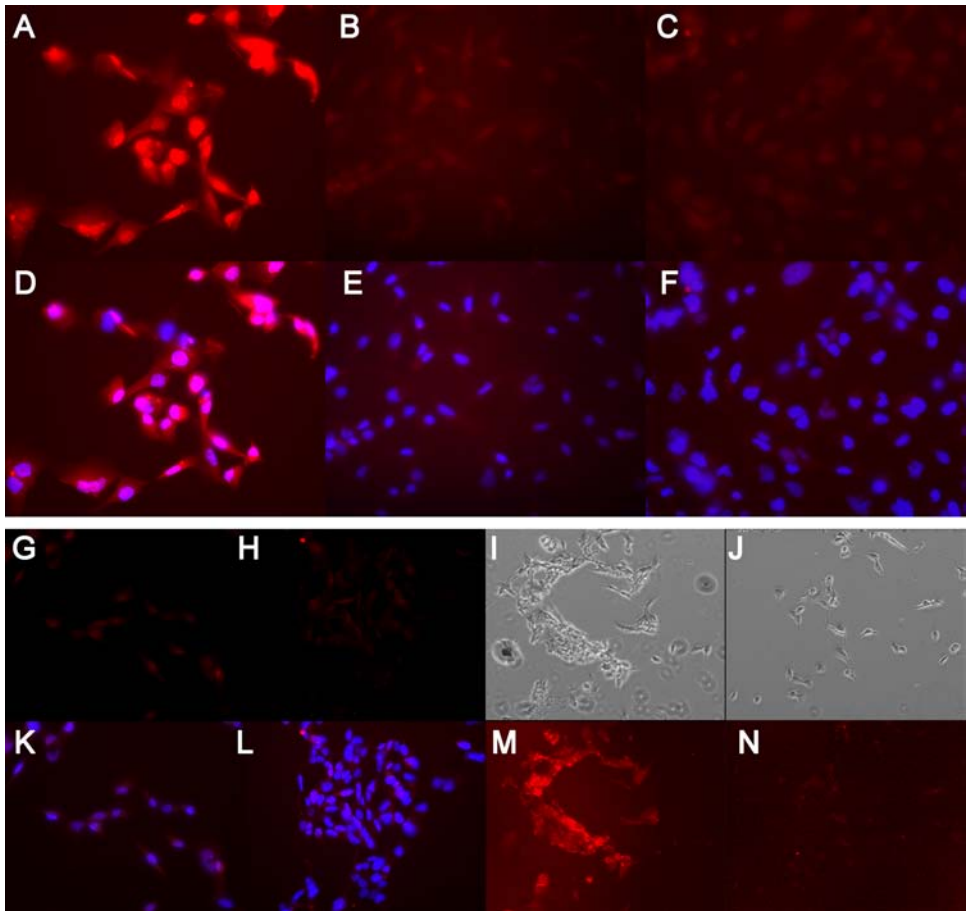

Figure 5. Tracer binding studies of Cy 5.5-**21** and Cy 5.5-**23** on human breast cancer cell lines BT-549 and BT-20. Incubation with tracer Cy 5.5-**23** shows binding to BT-549 cells ((A) Cy 5.5, (D) Cy 5.5/DAPI merge), while Cy 5.5-**21** does not show any binding ((B) Cy 5.5, (E) Cy 5.5/DAPI merge). Also, binding of Cy 5.5-**23** to BT-20 cells could not be observed ((C) Cy 5.5, (F) Cy 5.5/DAPI merge). The specificity of binding of Cy 5.5-**23** can be concluded from the absence of binding of Cy 5.5 alone on BT-549 ((G) Cy 5.5, (K) Cy 5.5/DAPI merge) and BT-20 cells ((H) Cy 5.5, (L) Cy 5.5/DAPI merge) and from predosing experiments with bestatin on nonfixated cells. While Cy 5.5-**23** strongly binds to BT-549 cells in the absence of bestatin ((I) phase contrast, (M) Cy 5.5), its binding is inhibited with 100-fold excess of bestatin (J) phase contrast, (N) Cy 5.5).

stage I without adverse toxic effects.[32] APN also exhibits a high affinity to peptides containing the amino acid motif asparagine−glycine−arginine (NGR). In a therapeutic approach, a conjugate of a truncated mutant form of human coagulation-inducing protein tissue factor and an NGR-containing peptide was demonstrated to selectively inhibit tumor perfusion during first-in-man studies.[33] APN inhibitors for therapeutic applications are developed since the early 1990s. A number of thiol-containing derivatives have been shown to have a high affinity to APN.[34−36] Xu and co-workers have described the synthesis of several nonpeptidic compounds, summarized in a recent concise review.[37] Many of the developed compounds contain a hydroxamic acid moiety, a common structural element for chelating bivalent cations like Zn^{2+}. The lead structure **I2** has been introduced by Xu and Li in 2005 and was described to have affinities in the low nanomolar range.[31] Our investigations utilizing the turnover of MCA as substrate for monitoring APN activity yielded micromolar inhibitory values for **I2**, **22**, and **23**.

We found that the different substitution patterns of precursor compounds **21**−**23** influence target affinity. Compounds **22** and **23** are substituted at the benzoyl moiety, while **21** is substituted at the cinnamoyl moiety. This results in a higher affinity of **22** and **23** to APN, which is also comparable to that of the lead **I2**. In contrast, **21** only exhibits a negligible affinity to APN. Additionally, this difference in reactivity could also be observed in cell growth inhibition examinations, where **21** behaved significantly different compared to **22** or **23**, which showed a well-defined inhibitory effect on APN-positive BT-549 cell growth. This stepwise, concentration-dependent cell growth toxicity displayed by **22** and **23** can probably be attributed to specific inhibition of APN. The toxicity of the fluorescent dye Cy 5.5 alone on cells was negligible on BT-549 cells and marginal on BT-20 cells. In the literature, there is not much data on Cy 5.5 toxicity, a comparison to ICG with an LD_{50} of 50 mg/kg in mice[38] shows that presumably there exists a large dosage window. To more closely evaluate the highly toxic but presumably not APN-dependent effect of **21** on cells, we tested the potencies of our precursor compounds **21**−**23** toward matrix metalloproteinases (MMPs −2, −8, −9, and −13), which also possess a Zn^{2+} cation at their active site, but an inhibition of MMP activity could not be observed (data not shown). This is in contrast to findings from Zhang and co-workers, who introduce **I2** and related compounds as gelatinase inhibitors with nanomolar affinities.[18,39]

Optical imaging is a desirable technique for in vivo diagnostics because it is a highly sensitive, inexpensive imaging method that can potentially resolve relevant target structures in vivo.[40,41] Optical imaging allows specific tagging of particular receptors,[42] antibodies,[43] genes, [44] or drugs,[45] thereby

measuring compound biodistribution and pharmacokinetics and hence leading to a better understanding of these processes. Fluorescence reflectance imaging (FRI) and fluorescence mediated tomography (FMT) as emerging optical imaging techniques have been shown to be capable of resolving fluorescence signatures three-dimensionally and (semi)-quantitatively.[46] For the design of APN target-specific fluorochromes, an APN ligand has to be combined with a fluorescent dye. In an optimal setting, the attachment of the dye to the ligand molecule does not alter or influence the binding properties of the ligand. Because of the apparent differences between **21** and **23**, we chose to label both compounds in order to more closely evaluate their different behavior. The resulting tracers Cy 5.5-**21** and Cy 5.5-**23** were tested in vitro on BT-549 and BT-20 cells, where the apparent differences of the two compounds were also observed. Human breast cancer cell line BT-549 binds Cy 5.5-**23** but not Cy 5.5-**21**. Predosing experiments with bestatin as a blocking agent suggest specific binding of Cy 5.5-**23** to APN on the cell surface, supporting the findings from cell toxicity examinations and confirming the assumption that dye modification of **23** does not disrupt target binding.

■ CONCLUSION

In conclusion, to the best of our knowledge, we here report for the first time the synthesis and characterization of a nonpeptidic, small-molecular fluorescent tracer with high affinity to aminopeptidase N (APN/CD13). The in vitro evaluation of this tracer shows promising results because of its high specificity to the target structure and a low residual (= non-APN-mediated) toxicity. These favorable characteristics will now be further evaluated in in vivo experiments with murine models of high APN expression. Further improvement of the tracer, including spacer-length, hydrophilicity, and flexibility and careful characterization of APN/CD13 expression levels in tissues, will warrant better understanding of APN pathophysiology.

■ AUTHOR INFORMATION

Corresponding Author

*Phone: +49 251 8356156. Fax: +49 251 8352067. E-mail: carsten.hoeltke@uni-muenster.de.

Notes

The authors declare no competing financial interest.

■ ACKNOWLEDGMENTS

Financial support by the German Research Foundation (Deutsche Forschungsgemeinschaft, DFG), Sonderforschungsbereich SFB 656, subprojects A4 and C6, and from the Interdisciplinary Center for Clinical Research (Interdisziplinäres Zentrum für Klinische Forschung, IZKF, Core-Units OPTI and SmAP) is gratefully acknowledged. We thank Marlena Brink, Ingrid Otto-Valk, Klaudia Niepagenkämper, and Ina Winkler for technical assistance.

■ REFERENCES

(1) Carmeliet, P. (2003) Angiogenesis in health and disease. *Nature Med. 9*, 653−660.

(2) Folkman, J. (2007) Angiogenesis: an organizing principle for drug discovery? *Nature Rev. Drug Discovery 6*, 273−286.

(3) Dixon, J., Kaklamanis, L., Turley, H., Hickson, I. D., Leek, R. D., Harris, A. L., and Gatter, K. C. (1994) Expression of aminopeptidase-n (CD 13) in normal tissues and malignant neoplasms of epithelial and lymphoid origin. *J. Clin. Pathol. 47*, 43−47.

(4) Kehlen, A., Gohring, B., Langner, J., and Riemann, D. (1998) Regulation of the expression of aminopeptidase A, aminopeptidase N/CD13 and dipeptidylpeptidase IV/CD26 in renal carcinoma cells and renal tubular epithelial cells by cytokines and cAMP-increasing mediators. *Clin. Exp. Immunol. 111*, 435−441.

(5) Surowiak, P., Drag, M., Materna, V., Suchocki, S., Grzywa, R., Spaczynski, M., Dietel, M., Oleksyszyn, J., Zabel, M., and Lage, H. (2006) Expression of aminopeptidase N/CD13 in human ovarian cancers. *Int. J. Gynecol. Cancer 16*, 1783−1788.

(6) Terauchi, M., Kajiyama, H., Shibata, K., Ino, K., Nawa, A., Mizutani, S., and Kikkawa, F. (2007) Inhibition of APN/CD13 leads to suppressed progressive potential in ovarian carcinoma cells. *BMC Cancer 7*, 140.

(7) Iguchi, K., Nakano, T., Usui, S., and Hirano, K. (2006) Incadronate inhibits aminopeptidase N expression in prostatic PC-3 cells. *Cancer Lett. 237*, 223−233.

(8) Ishii, K., Usui, S., Sugimura, Y., Yoshida, S., Hioki, T., Tatematsu, M., Yamamoto, H., and Hirano, K. (2001) Aminopeptidase N regulated by zinc in human prostate participates in tumor cell invasion. *Int. J. Cancer 92*, 49−54.

(9) Riemann, D., Gohring, B., and Langner, J. (1994) Expression of aminopeptidase N/CD13 in tumour-infiltrating lymphocytes from human renal cell carcinoma. *Immunol. Lett. 42*, 19−23.

(10) Stange, T., Kettmann, U., and Holzhausen, H. J. (2000) Immunoelectron microscopic demonstration of the membrane proteases aminopeptidase N/CD13 and dipeptidyl peptidase IV/CD26 in normal and neoplastic renal parenchymal tissues and cells. *Eur. J. Histochem. 44*, 157−164.

(11) Kehlen, A., Lendeckel, U., Dralle, H., Langner, J., and Hoang-Vu, C. (2003) Biological significance of aminopeptidase N/CD13 in thyroid carcinomas. *Cancer Res. 63*, 8500−8506.

(12) Severini, G., Gentilini, L., and Tirelli, C. (1991) Diagnostic evaluation of alanine aminopeptidase as serum marker for detecting cancer. *Cancer Biochem. Biophys. 12*, 199−204.

(13) Bhagwat, S. V., Lahdenranta, J., Giordano, R., Arap, W., Pasqualini, R., and Shapiro, L. H. (2001) CD13/APN is activated by angiogenic signals and is essential for capillary tube formation. *Blood 97*, 652−659.

(14) Bhagwat, S. V., Petrovic, N., Okamoto, Y., and Shapiro, L. H. (2003) The angiogenic regulator CD13/APN is a transcriptional target of Ras signaling pathways in endothelial morphogenesis. *Blood 101*, 1818−1826.

(15) Hashida, H., Takabayashi, A., Kanai, M., Adachi, M., Kondo, K., Kohno, N., Yamaoka, Y., and Miyake, M. (2002) Aminopeptidase N is involved in cell motility and angiogenesis: its clinical significance in human colon cancer. *Gastroenterology 122*, 376−386.

(16) von Wallbrunn, A., Waldeck, J., Höltke, C., Zühlsdorf, M., Mesters, R., Heindel, W., Schäfers, M., and Bremer, C. (2008) In vivo optical imaging of CD13/APN-expression in tumor xenografts. *J. Biomed. Opt. 13*, 011007.

(17) Höltke, C., von Wallbrunn, A., Kopka, K., Schober, O., Heindel, W., Schäfers, M., and Bremer, C. (2007) A fluorescent photoprobe for the imaging of endothelin receptors. *Bioconjugate Chem 18*, 685−694.

(18) Li, X., Li, Y., and Xu, W. (2006) Design, synthesis, and evaluation of novel galloyl pyrrolidine derivatives as potential anti-tumor agents. *Bioorg. Med. Chem. 14*, 1287−1293.

(19) van Hensbergen, Y., Broxterman, H. J., Hanemaaijer, R., Jorna, A. S., van Lent, N. A., Verheul, H. M., Pinedo, H. M., and Hoekman, K. (2002) Soluble aminopeptidase N/CD13 in malignant and nonmalignant effusions and intratumoral fluid. *Clin. Cancer Res. 8*, 3747−3754.

(20) Tahtaoui, C., Parrot, I., Klotz, P., Guillier, F., Galzi, J. L., Hibert, M., and Ilien, B. (2004) Fluorescent pirenzepine derivatives as potential bitopic ligands of the human M1 muscarinic receptor. *J. Med. Chem. 47*, 4300−4315.

(21) Cai, W., and Chen, X. (2008) Multimodality molecular imaging of tumor angiogenesis. *J. Nucl. Med. 49* (Suppl2), 113S−128S.

(22) Backer, M. V., Levashova, Z., Patel, V., Jehning, B. T., Claffey, K., Blankenberg, F. G., and Backer, J. M. (2007) Molecular imaging of VEGF receptors in angiogenic vasculature with single-chain VEGF-based probes. *Nature Med. 13*, 504−509.
(23) Beer, A. J., and Schwaiger, M. (2008) Imaging of integrin alphavbeta3 expression. *Cancer Metastasis Rev 27*, 631−644.
(24) Pasqualini, R., Koivunen, E., and Ruoslahti, E. (1995) A peptide isolated from phage display libraries is a structural and functional mimic of an RGD-binding site on integrins. *J. Cell Biol. 130*, 1189−1196.
(25) Beer, A. J., Kessler, H., Wester, H. J., and Schwaiger, M. (2011) PET Imaging of Integrin alphaVbeta3 Expression. *Theranostics 1*, 48−57.
(26) Lanzardo, S., Conti, L., Brioschi, C., Bartolomeo, M. P., Arosio, D., Belvisi, L., Manzoni, L., Maiocchi, A., Maisano, F., and Forni, G. (2011) A new optical imaging probe targeting alphaVbeta3 integrin in glioblastoma xenografts. *Contrast Media Mol. Imaging 6*, 449−458.
(27) Ye, Y., Bloch, S., Xu, B., and Achilefu, S. (2006) Design, synthesis, and evaluation of near infrared fluorescent multimeric RGD peptides for targeting tumors. *J. Med. Chem. 49*, 2268−2275.
(28) Beer, A. J., Haubner, R., Sarbia, M., Goebel, M., Luderschmidt, S., Grosu, A. L., Schnell, O., Niemeyer, M., Kessler, H., Wester, H. J., Weber, W. A., and Schwaiger, M. (2006) Positron emission tomography using [18F]Galacto-RGD identifies the level of integrin alpha(v)beta3 expression in man. *Clin. Cancer Res. 12*, 3942−3949.
(29) Buehler, A., van Zandvoort, M. A., Stelt, B. J., Hackeng, T. M., Schrans-Stassen, B. H., Bennaghmouch, A., Hofstra, L., Cleutjens, J. P., Duijvestijn, A., Smeets, M. B., de Kleijn, D. P., Post, M. J., and de Muinck, E. D. (2006) cNGR: a novel homing sequence for CD13/APN targeted molecular imaging of murine cardiac angiogenesis in vivo. *Arterioscler. Thromb. Vasc. Biol. 26*, 2681−2687.
(30) Bauvois, B., and Dauzonne, D. (2006) Aminopeptidase-N/CD13 (EC 3.4.11.2) inhibitors: chemistry, biological evaluations, and therapeutic prospect. *Med. Res. Rev. 26*, 88−130.
(31) Xu, W., and Li, Q. (2005) Progress in the development of aminopeptidase N (APN/CD13) inhibitors. *Curr. Med. Chem.: Anticancer Agents 5*, 281−301.
(32) Ichinose, Y., Genka, K., Koike, T., Kato, H., Watanabe, Y., Mori, T., Iioka, S., Sakuma, A., and Ohta, M. (2003) Randomized double-blind placebo-controlled trial of bestatin in patients with resected stage I squamous-cell lung carcinoma. *J. Natl. Cancer Inst. 95*, 605−610.
(33) Bieker, R., Kessler, T., Schwöppe, C., Padro, T., Persigehl, T., Bremer, C., Dreischaluck, J., Kolkmeyer, A., Heindel, W., Mesters, R. M., and Berdel, W. E. (2009) Infarction of tumor vessels by NGR-peptide-directed targeting of tissue factor: experimental results and first-in-man experience. *Blood 113*, 5019−5027.
(34) Fournie-Zaluski, M. C., Coric, P., Turcaud, S., Bruetschy, L., Lucas, E., Noble, F., and Roques, B. P. (1992) Potent and systemically active aminopeptidase N inhibitors designed from active-site investigation. *J. Med. Chem. 35*, 1259−1266.
(35) Chauvel, E. N., Llorens-Cortes, C., Coric, P., Wilk, S., Roques, B. P., and Fournie-Zaluski, M. C. (1994) Differential inhibition of aminopeptidase A and aminopeptidase N by new beta-amino thiols. *J. Med. Chem. 37*, 2950−2957.
(36) Chen, H., Roques, B. P., and Fournie-Zaluski, M. C. (1999) Design of the first highly potent and selective aminopeptidase N (EC 3.4.11.2) inhibitor. *Bioorg. Med. Chem. Lett. 9*, 1511−1516.
(37) Zhang, X., Fang, H., Zhang, J., Yuan, Y., and Xu, W. (2011) Recent advance in aminopeptidase N (APN/CD13) inhibitor research. *Curr. Med. Chem. 18*, 5011−21.
(38) Alford, R., Simpson, H. M., Duberman, J., Hill, G. C., Ogawa, M., Regino, C., Kobayashi, H., and Choyke, P. L. (2009) Toxicity of organic fluorophores used in molecular imaging: literature review. *Mol. Imaging 8*, 341−354.
(39) Zhang, L., Zhang, J., Fang, H., Wang, Q., and Xu, W. (2006) Design, synthesis and preliminary evaluation of new cinnamoyl pyrrolidine derivatives as potent gelatinase inhibitors. *Bioorg. Med. Chem. 14*, 8286−8294.
(40) Bremer, C., Ntziachristos, V., Mahmood, U., Tung, C. H., and Weissleder, R. (2001) Progress in optical imaging. *Radiologe 41*, 131−137.
(41) Ntziachristos, V., Bremer, C., Graves, E. E., Ripoll, J., and Weissleder, R. (2002) In vivo tomographic imaging of near-infrared fluorescent probes. *Mol. Imaging 1*, 82−88.
(42) Chen, W. T., Khazaie, K., Zhang, G., Weissleder, R., and Tung, C. H. (2005) Detection of dysplastic intestinal adenomas using a fluorescent folate imaging probe. *Mol. Imaging 4*, 67−74.
(43) Ballou, B., Fisher, G. W., Waggoner, A. S., Farkas, D. L., Reiland, J. M., Jaffe, R., Mujumdar, R. B., Mujumdar, S. R., and Hakala, T. R. (1995) Tumor labeling in vivo using cyanine-conjugated monoclonal antibodies. *Cancer Immunol. Immunother. 41*, 257−263.
(44) Bremer, C., and Weissleder, R. (2001) In vivo imaging of gene expression. *Acad. Radiol. 8*, 15−23.
(45) Arttamangkul, S., Alvarez-Maubecin, V., Thomas, G., Williams, J. T., and Grandy, D. K. (2000) Binding and internalization of fluorescent opioid peptide conjugates in living cells. *Mol. Pharmacol. 58*, 1570−1580.
(46) Ntziachristos, V., Bremer, C., and Weissleder, R. (2003) Fluorescence imaging with near-infrared light: new technological advances that enable in vivo molecular imaging. *Eur. Radiol. 13*, 195−208.
(47) Li, X., Wang, Y., Wu, J., Li, Y., Wang, Q., and Xu, W. (2009) Novel aminopeptidase N inhibitors derived from antineoplaston AS2−5 (Part II). *Bioorg. Med. Chem. 17*, 3061−3071.
(48) Fieser, L. F., and Fieser, M. (1967) *Reagents for Organic Synthesis* p 478, Vol. *1*, Wiley, New York.